Environmental risk of severely Pb-contaminated riverbank sediment as a consequence of hydrometeorological perturbation

SFL Lynch[1*], LC Batty[1], P Byrne[2]

[1] School of Geography, Earth and Environmental Sciences, University of Birmingham, Edgbaston, Birmingham, B15 2TT, UK: E-mail: l.c.batty@bham.ac.uk

[2] School of Natural Scieces and Psychology, Liverpool John Moores University, Byrom Street, Liverpool, L3 3AF, UK; E-mail: p.a.byrne@ljmu.ac.uk

[*] Author to whom correspondence should be addressed: AECOM, Floor 4, Bridgewater House, Whitworth St, Manchester, M1 6LT; E-mail: Sarah.Lynch@AECOM.com

Keywords: Mining, pollution, Pb, diffuse pollution, metal, contamination, sediment, riverbank

1. Introduction

Metal mining activities including mineral extraction, processing and dumping of contaminated waste alongside river channels has resulted in the widespread metal pollution of soils and sediments and is a worldwide health concern (Foulds et al 2014; Zhang et al 2012; Zadnik 2010). The impacts of these activities have been reported internationally; Coeur d'Alene River Valley, Idaho (USGS 2001), San Luis, Argentina (Tripole et al 2006) and throughout Europe, Upper Silesia in southern Poland (Ullrich et al. 1999), Iberian Pyrite Belt, south west Spain (Torres et al 2013). In England and Wales, mining impacted catchments play a critical role in the distribution of metals through fluvial systems with the highest metal flux arising from mineralised catchments with a history of metal mining (Mayes et al. 2013). Contrary to the traditional focus on point sources of pollution from adits and shafts, a greater emphasis has been placed on dealing with diffuse forms, primarily due to the EU Water Framework Directive 2000/60/EC requirement that management of water quality should be at a catchment scale delivered through the river basin management plans (Collins et al. 2012). There are 226 waterbodies categorised as 'impacted' by non-coal mine water pollution in England and Wales and over 50% show evidence of diffuse pollution (Environment Agency 2010). That could serve as a barrier to achieving 'good' surface water chemical status for all water bodies by 2021 (EU amending directives 2000/60/EC and 2008/105/EC). Identifying the exact sources, and understanding pollution dynamics, within a catchment are listed as key priorities for effective management and remediation efforts (Environment Agency 2012a).

Pb is listed as a priority substance in EU amending directives 2000/60/EC and 2008/105/EC in the field of water policy because of its known toxic effects. Unlike elements, such as Cu and Zn, Pb has no known biological function and therefore can be harmful to flora and fauna at very low levels (Chibuike and Obiora 2014). Pb is bioaccumulative, passing through trophic levels of the food chain and increasing in concentration at each level. Bioavailable forms of Pb can be taken up and stored in tolerant plants (Sharma and Dubey 2005) and macroinvertebrates (Cid et al. 2010), accumulate in earthworms (Wijayawardena et al. 2017) and high concentrations can be stored in liver, kidneys and muscles of cattle due to the consumption of contaminated forage (Zadnik 2010). In severely contaminated mining catchments such as Coeur d'Alene river Basin, USA, levels of Pb in children's blood have been found to far exceed federal intervention levels (USGS 2001). Pb can have chronic

55 and acute toxicity effects that include detrimentally impacting macroinvertebrate community structure
56 (Montserrat 2010; Byrne et al. 2013), phytotoxicity resulting in riverbank instability (Environment
57 Agency 2008), chronic effects in cattle such as osteoporosis and anaemia with high exposure
58 resulting in ataxia and death (Zadnik 2010) and neurotoxic effects in children such as behaviour
59 problems, lower IQ and learning disabilities (Wijayawardena et al 2017).

60 In mining impacted catchments Pb can be introduced into the environment when primary sulphide
61 mineral galena (PbS) is brought to the surface and oxidised through exposure to atmospheric
62 conditions. High concentrations of Pb and sulphate can be released into fluvial systems in this way.
63 Once introduced to the river system Pb can be transported downstream as a free ion, aqueous
64 complex, or in particulate form sorbed to sediment particles (vanLoon and Duffy 2011). Where
65 physical, chemical and hydrological changes within the river allow, Pb associated sediment would be
66 deposited on riverbanks and floodplains, the location depending on factors such as particle size, flood
67 magnitude and morphology of the river (Macklin and Dowsett 1989; Bradley 1995; Dennis et al.
68 2003). The partitioning of Pb in sediment is dependent on the chemical environmental conditions and
69 the geology, for example formations high in quartz or carbonates that would influence mineralogy.
70 Where Pb is associated with mineral forms impervious to weathering, environmental changes would
71 not influence the mobilisation of dissolved Pb and this contaminant would remain unavailable for
72 uptake. However in mining impacted catchments Pb is often associated with Fe and Mn (hydr)oxide
73 and sulphur minerals in the sediment (Tripole et al 2006; Buekers et al 2008; Zakir and Shikazono
74 2011). These minerals can undergo dissolution and precipitation reactions in response to dynamic
75 changes in redox potential, pH (Nordstrom and Alpers 1999) and levels of moisture (Buckby et al.
76 2003) – processes that commonly occur within the riverbank environment (Byrne et al. 2013; Krause
77 et al. 2010; Du Laing et al. 2009). As a result the sediment can become a source of dissolved Pb to
78 river systems (Charlatchka and Cambier 2000; Torres et al 2013).

79 Climate projections based on UKCP09 river basin regions in West Wales and North West England
80 (Met Office 2017) indicate a shift towards aridity by 2020. Summer river flows are expected to decline
81 and Q95 (flow that is exceeded 95% of the time) may reduce 26% by 2050 and 35% by 2080 in
82 western Wales, using medium emissions (P50) scenarios (DEFRA 2012a). Furthermore projections
83 indicate a rise in the occurrence of localized heavy rainfall events, particularly in winter. Peak river

flows are expected to increase 13% by 2020, 20.8% by 2050 and 27.6% by 2080 in Wales, using medium (P50) scenarios (DEFRA 2012b). Changes in river flow alter river stage and expose river bank sediments to variable water saturation regimes, periods of inundation are followed by periods of drainage. If climate change projections are correct, patterns of inundation and drainage are likely to become more pronounced. The focus of the current research is within the UK, however it is important to note that climate driven changes in distribution of rainfall and the resulting increase in peak flow events within mining impacted systems, is an issue experienced internationally (Ciszewski and Grygar 2016).

The current research is intended to add to the work of Lynch et al. (2017) in which the geochemical mechanisms controlling dissolved Zn release from riverbank sediments were determined (Lynch et al. 2017). Key Zn control mechanisms were: The (co)precipitation of Zn with Mn (hydroxides), followed by the reductive dissolution and release of Zn in response to prolonged flooding and; Precipitation of Zn sulphate salts over long dry antecedent periods followed by the immediate dissolution of these salts and release of dissolved Zn on sediment flood wetting.

In the current study the same mesocosm experiments are run to allow the authors to determine the control that different sequential patterns of flooding and drainage have on the mobilisation of dissolved Pb. Pb is reported as less mobile than Zn under oxic conditions (Galan et al. 2003; Carroll et al. 1998) with a greater affinity for Fe (hydr)oxide surfaces (Evans 1991; Wang 2010) and a lower sorption edge (Lee et al 2002; Appelo and Postma 2010). However, in severely polluted catchments contaminated sediments have been identified as an important source of dissolved Pb contamination to surface water (Palumbo-Roe et al 2012; Byrne et al 2013) and it is hypothesised that certain flood/drain sequences will control the mobilisation of dissolved Pb from contaminated riverbank sediment.

Key hydrogeochemical mechanisms may include: (i) Pb co-precipitation with and sorption to Fe/Mn (hydr)oxides under oxidised (drained) periods followed by reductive dissolution and release of dissolved Pb due to a fall in redox potential conditions over prolonged flood periods; (ii) the oxidation of the primary mineral galena and release of dissolved Pb and sulphate where previously reduced sediment is exposed to oxic conditions (Wragg and Palumbo-Roe 2011) (iii) the precipitation of insoluble Pb sulphides due to a fall in redox potential conditions over prolonged flood periods (Lynch

et al 2014); (iv) control of dissolved Pb concentrations to low levels through saturation with respect to anglesite ($PbSO_4$) over flooded periods (Palumbo-Roe et al. 2013; Appelo and Postma 2010); (v) hydrological saturation and precipitation of soluble sulphate salts over long dry periods followed by dissolution of these salts, and a 'flush' of dissolved Pb and sulphate, in response to flood wetting (Byrne et al. 2013).

Previous studies have investigated the effects of alternately flooding and drying contaminated soil for different frequencies and durations on the mobilisation of toxic trace elements such as Cd and Zn (Lynch et al 2017; Shaheen et al 2014; Du Laing et al 2007). This study is unique in that experiments examine the patterns of dissolved Pb release from coarse grained riverbank sediment collected from a mining impacted catchment highly contaminated with Pb. Understanding the mechanisms of release for this toxic metal under varying hydrometeorological perturbations is crucial information for environmental monitoring and the development of successful pollution control measures.

To establish the environmental risk Pb-contaminated riverbank sediment may pose in light of UK climate projections, the results of two laboratory mesocosm experiments are examined. The objectives were to: (i) Investigate if flooding and draining sequences influence the patterns of dissolved Pb release from severely contaminated river bank sediment; (ii) Identify key hydrogeochemical processes responsible for controlling the mobilisation of dissolved Pb and if they differ from the mechanisms of control for dissolved Zn; (iii) Establish if Pb contaminated riverbank sediment poses an environmental risk when exposed to alternate flooding and draining sequences;

2. Introduction

A summary of the sample site data and mesocosm treatment methods is provided below. Please see (Lynch et al. 2017) for detailed information on the methodology.

2.1 Sediment sample site

The sample site at Cwmystwyth (SN799743) is located in central Wales, at an elevation of 250 m above sea level (ASL). The mine site is drained by the Afon Ystwyth River which runs from east to west, draining into the Irish Sea at Aberystwyth (approximately 25 km north east of Cwmystwyth) (Fig1). The north side of the river is marked by spoil heaps rising to 500 m ASL and on the south side grass banks, used primarily for grazing, rise steeply to 450 m ASL. Mining ceased at Cwmystwyth in 1921 (Bick

1976). The country rock dates from the Silurian period with alternating bedrock of hard coarse sandstones and shales that form the upper Llandovery Series (British Geological Survey 2007). Rivers that rise on this type of geology have been described as 'Base Poor' having a low alkalinity, so less able to buffer acidic inputs (Natural Resources Wales 2004).

2.2 Rainfall and river flow characteristics

Detailed information on rainfall and flow at the sample site can be found in Lynch et al (2017). Generally flow rises and recedes quickly, however extended periods (greater than a week) of flow well above the mean value (1.989 m^3/s) (leading to riverbank and floodplain inundation) and extended periods well below the mean value (leading to drainage and exposure of riverbank and floodplain), are common (Centre for Ecology and Hydrology 2015). Changes in river flow are known to cause a rise and fall in river stage that can influence patterns of hyporheic exchange flow (Byrne et al. 2013).

Fig. 1 Location of sample site, grid reference SN799743 (denoted by a star) at the Cwmystwyth abandoned mine complex in the River Ystwyth catchment in mid-Wales (inset)

158 **2.3 Sediment collection**

159 Sediment was collected on two occasions, July 2012 and December 2013 for analysis in two separate
160 mesocosm treatments. Visual inspection of the northern riverbank indicated that sediment was made
161 up of predominantly sandy gravel interspersed with some finer silt particles and larger pebbles and
162 boulders. The sediment samples were collected from the north bank of the river at the same site, but
163 different locations. On the first visit, sediment was taken from waste piles running along the side of the
164 river channel. This material would have been dumped along the side of the river during active mining
165 and was therefore likely to contain high concentrations of primary and secondary minerals. On the
166 second visit, material was taken from the base of the mining waste piles, on a lateral flow path, so
167 was likely to contain lower concentrations of the primary waste and material eroded from the waste
168 piles. This site was closer to the active river channel and therefore would be more susceptible to
169 hydrometeorological perturbations. A stainless steel shovel was used to collect sediment from the top
170 10 cm.

171 **2.4 Laboratory analysis**

172 ***2.4.1 Mesocosm experiments***

173 Two mesocosm experiments were conducted in order to meet the objectives. The first experiment was
174 run to determine the effect alternately wetting and drying contaminated sediment for different durations
175 and frequencies had on the release of dissolved Pb and establish whether the sediment posed an
176 environmental risk. The second experiment focused on runs where patterns of dissolved Pb release
177 were pronounced allowing a (i) comparison of concentration and lability of Pb in the sediment at the two
178 different sampling locations; (ii) comparison of the environmental risk the sediment posed at each
179 location (iii) determination of the repeatability of the results. For both experiments water and sediment
180 analysis enabled the elucidation of the key geochemical mechanisms of dissolved Pb mobilisation.
181 The sediment was homogenised by hand and larger pebbles were removed. The sediment was then
182 packed into each mesocosm to a depth of 24 cm using a plastic trowel (Fig. 2). An extended
183 experimental timeframe for each column of 20 days at field capacity, to equilibrate the sediment,
184 followed by a maximum of 11 weeks treatment period promoted the removal of any artefacts and
185 allowed time for systems to settle into a steady pattern. Artificial Rainwater (ARW) was created based
186 on Plynlimon rainwater chemistry (pH 4.9 - 5.2), found in the uplands of mid-Wales (Neal et al. 2001).
187 For field capacity, twice a week, 500 ml of ARW was added via the top of the mesocosm until water

188 percolated though the bottom tap (Fig. 2). Following field capacity, mesocosms were divided into 7
189 different treatments. 5 were variable wet and dry runs and 2 constant controls. The Cwmystwyth gauged
190 daily flow (grid reference SN790737), taken from the UK National River Flow Archive (Centre for
191 Ecology and Hydrology 2015), provided guidance regarding the length of time riverbank sediment may
192 be exposed to atmosphere or submerged (section 2.2). Variable runs were designed to include longer
193 wet runs, longer dry runs and wet and dry run of same duration and frequency. Control runs were non-
194 variable and either constant wet (flood) or unsaturated and oxidised (field capacity). This allowed a
195 comparison between variable and non-variable wet and dry runs. Constant flood and field capacity were
196 sampled every week. Variable run samples were taken only at the start and end of a wet period. Runs
197 were: 1 week wet followed by 1 week dry (1wwet), 1 week wet followed by 2 weeks dry (2wdry), 1 week
198 wet followed by 3 weeks dry (3wdry), 2 weeks wet followed by 1 week dry (2wwet), 3 weeks wet followed
199 by 1 week dry (3wwet), Flood (Flood) and field capacity (F/C). The temperature was maintained at 22-
200 23ºC for the 1st mesocosm experiment and ~18ºC for the 2nd mesocosm experiment.
201 Water samples were taken from the top of the mesocosm using a plastic syringe and from the bottom
202 via a tap, in that order to avoid mixing between levels and filtered through a 0.45 µm PTFE syringe filter.
203 A Hanna Combo pH/EC and temperature hand held stick meter model No 98129, recorded pH,
204 conductivity and temperature for each sample. An Aquaread Aquameter multiparameter water quality
205 probe was used to measure dissolved oxygen (DO) and redox potential (ORP) (2nd mesocosm
206 experiment only). The ORP reference electrode was type 3MPK1 AgCl and ORP readings were
207 converted to the hydrogen scale (Eh) as instructed by Aquaread. For further detail regarding mesocosm
208 methodology, please see Lynch et al. (2017).
209
210

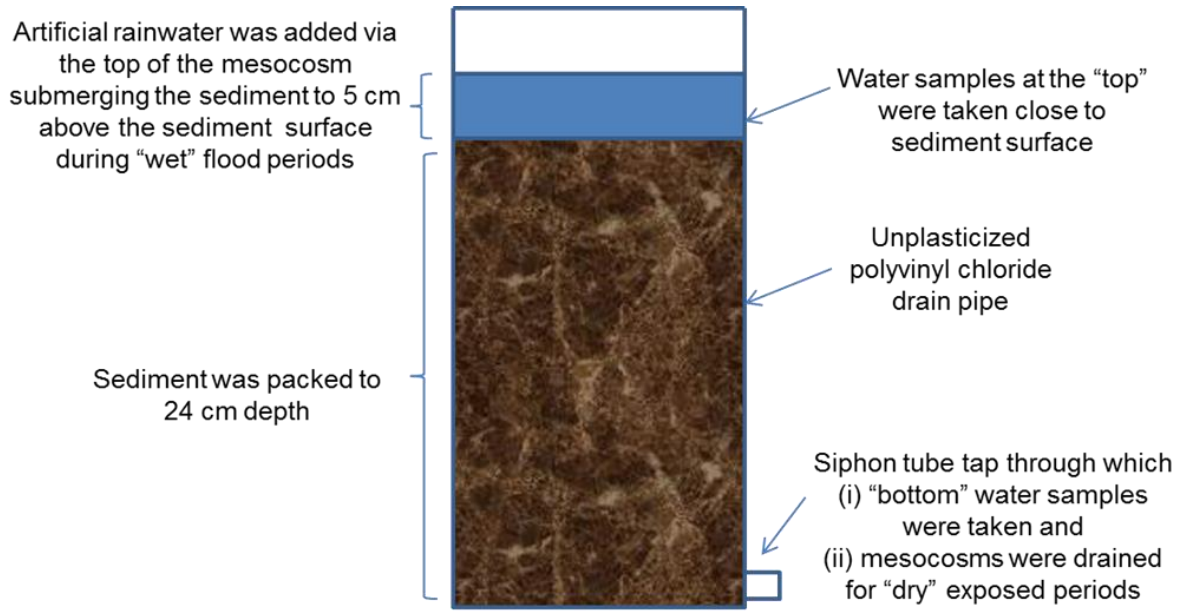

211
212

213 Fig. 2 Outline of mesocosm including sampling points

214 *Note: Filtered samples are referred to as 'dissolved' concentrations. However, this is operationally*
215 *defined and the authors acknowledge that the samples may contain colloidal and/or nano-sized*
216 *particles.*

217 ***2.4.2 Trace metal and anion analysis***

218 Flame Atomic Absorption Spectroscopy (FAAS) (Perkin Elmer Analyst 300) was used to measure Fe,
219 Mn, Pb, Ca, Ni, Cu (mg l^{-1}) in filtered pore water samples from the 1st mesocosm experiment. Detection
220 limits were: Ca, 0.06; Fe, 0.03; Cu, 0.01; Mn, 0.01; Pb, 0.04 and Ni, 0.01 (mg l^{-1}). Inductively Coupled
221 Plasma with Optical Emission Spectroscopy (ICP/OES) (iCAP 6500 Duo) was used to measure
222 dissolved Fe, Mn and Pb in (i) filtered pore water samples of the 2nd mesocosm experiment and (ii)
223 sequential extraction samples from the 1st and 2nd mesocosm experiments. Detection limits were: Fe,
224 0.005; Mn, 0.001; Pb, 0.05 (mg l^{-1}). Ion Chromatography (Dionex ICS2000) was used to measure
225 dissolved sulphate, nitrate, chloride and phosphate in pore water samples of the 1st mesocosm
226 experiment and the 2nd mesocosm experiment. Detection limits were: sulphate, 0.07; nitrate, 0.04;
227 chloride, 0.06; phosphate, 0.06 (mg l^{-1}). Flame photometer BWB technologies was used for detection
228 of Na, K and Ca in filtered pore water of the 2nd mesocosm experiment. For all analysis quality control
229 standards and blanks, either de-ionised water, or matrix matched solutions for sequential extractions,
230 were used throughout. The results were considered acceptable if the data were within 5% of the
231 expected concentration.

232

2.4.3 Alkalinity and inorganic carbon analysis (water and sediments)

Unfiltered water samples from both mesocosm treatment runs were analysed for alkalinity (as calcium carbonate) using the standard operating procedure for Great Lakes National Program office total alkalinity titration method (US EPA 1992). Filtered pore water samples were tested for total carbon (TC) and non purgeable organic carbon (NPOC) using a carbon analyser (Shimadzu TOC-V CSN). Inorganic Carbon = Total Carbon – Non Purgeable Organic carbon. For non purgeable organic carbon the sample was first acidified to pH 2 to transform inorganic carbon to CO_2. The CO_2 was removed via sparging with a carrier gas. During this process some purgeable organic carbon (benzene, toluene, cyclohexane and chloroform) may be partly removed. Although there tends to be negligible amounts of these in surface water samples, the remaining organic carbon is "non-purgeable" and is measured, as mg (of carbon) per litre of water, through CO_2 detection in the analyser using a non-dispersive infrared (NDIR) detector. Standards and blanks were used throughout. The results were considered acceptable if within 5% of the expected concentration. Sediment collected for the 2nd mesocosm experiment was analysed for total inorganic (IC) using a separate solid sample module of the Shimadzu instrument (SSM 5000A). A sub sample of sieved (2 mm) sediment was weighed (no greater than 50 mg), and oven dried at 140^{o}C for 24 hours. The sample was treated with phosphoric acid inside the Shimadzu instrument to produce CO_2 that was purged at 200^{o}C and detected using a non-dispersive infrared (NDIR) detector. Calibration was performed using different weights of sodium carbonate containing 11.3% carbon. The results provided % TIC (Shimadzu Scientific Instruments, 2014). The results were considered acceptable if within 5% of the expected concentration.

2.4.4 Statistical analysis

All calculations were performed using SPSS 20.0. Statistical tests revealed the data was not normally distributed therefore significant differences in pore water data were identified through non-parametric Wilcoxon rank sum test. Relationships between Pb and pore water variables were determined using Spearman's rho 2-tailed non-directional tests.

To determine key factors linked to the mobilization of dissolved Pb for selected variable runs at the bottom of the mesocosms, Principal Component Analysis (PCA) was carried out. Data was assessed to ensure (i) that underlying variables correlated (Bartlett's test of sphericity) and (ii) sampling adequacy

263 (Kaiser-Meyer-Olkin). Factor rotation was chosen based on whether the factors (principal components
264 (PC)) were thought to be unrelated (orthogonal) or related (oblique). For further information on PCA
265 see supplementary information D.
266
267 ***2.4.5 PHREEQC (Ph-Redox-Equilibrium in "C")***
268 The geochemical computer program PHREEQC was used for speciation and saturation index (SI)
269 calculations using the WATEQ4F.dat database distributed with the PHREEQC program. The saturation
270 state of various minerals were calculated using input data derived from pore water measurements for
271 selected runs (Tables A1 and A2). Data was considered acceptable if charge balance was $\leq$ 5%.
272
273 In some cases the control of trace metal solutes by equilibrium with a mineral can be demonstrated
274 (Appelo and Postma, 2010). The keyword 'equilibrium_phases' was used to calculate the concentration
275 of anglesite that would precipitate and subsequent dissolved Pb concentrations in pore and surface
276 water if conditions were brought to equilibrium and reached saturation with respect to anglesite.
277
278 ***2.4.6 Sequential Extraction of sediment samples***
279 Dynamic changes in redox potential conditions can occur within river bank sediment due to flooding /
280 draining sequences (Lynch et al 2017; Lynch et al. 2014; Du Laing et al. 2009). Different Fe phases
281 display a wide range of reactivity (adsorption capacity and susceptibility to reduction). A fall in redox
282 potential conditions can result in the microbially mediated reductive dissolution of Fe and Mn
283 (hydroxides) (Stumm and Sulzberger 1992; Lynch et al. 2014). This can serve to remobilize
284 partitioned contaminants such as Pb (Torres et al. 2013). When flood waters subside the exposure of
285 previously reduced sediment surfaces to atmospheric conditions may result in the oxidation and
286 hydrolysis of previously reduced Fe and Mn (Lovley and Phillips 1989; Grundl and Delwiche 1993). Fe
287 and Mn (hydr)oxides can rapidly (minutes to hours) scavenge high concentrations of dissolved trace
288 metal contaminants such as Pb (Burton 2010, Caetano et al. 2003). In order to understand the
289 reactivity of Fe and Mn minerals in the sediment along with partitioned Pb and therefore the potential
290 for the sediment to control the mobilisation of Pb in response to dynamic changes in redox potential a
291 modified 4 step sequential extraction procedure was carried out in triplicate on sediments samples
292 collected for 1st and 2nd mesocosm experiments. The sequential extraction procedure focused

primarily on Fe and Mn minerals with steps run sequentially from 'most reactive' to 'least reactive'. Extractions were carried out on freeze dried -70ºC sediment (63 ≤ µm) (Table 1). Please see supplementary information 'E' for full extraction methodology.

Table 1 Sequential extraction steps

Step #	Extractant	Extraction details	References
1	0.5M HCl*	Rotational shaker for 1 hour, centrifuged, supernatant filtered (0.45µm)	Lovley and Phillips (1986)
2	0.25M hydroxylamine hydrochloride in 0.25M HCl	Rotational shaker for 1 hour, centrifuged, supernatant filtered (0.45µm)	Poulton and Cranfield (2005)
3	50 gL^{-1} sodium dithionate with 0.2M in 0.35M acetic acid	Rotational shaker for 2 hours, centrifuged, supernatant filtered (0.45µm)	Poulton and Cranfield (2005)
4	Aqua Regia cHCl and $cHNO_3$ (3:1 molar ratio)	Agitated gently overnight. Following day heated 80 ºC for 2 hours. Filtered Whatman no 42	Wilson and Pyatt (2007), Montserrat (2012)

0.5M HCl is a moderately corrosive first step and therefore it is not possible to differentiate the release of divalent ions from loosely sorbed/ exchangeable phase or as a result of dissolution of amorphous or soluble phases. Furthermore, the first step was originally used for analysis of Fe from within a different sediment environment. The implications regarding these points are included in the results/ discussion sectionas the authors consider the results provide valuable supporting data.

2.4.7 Scanning Electron Microscopy with Energy Dispersive X-ray Spectroscopy (SEM/EDX)

A combination of SEM/EDX was carried out to create images of and identify elements at the surface of the sediment samples for areas at micron scale. Freeze dried sediment was dusted lightly onto carbon stubs and coated in carbon to encourage conductivity. Samples were analysed with a Philips XL30 FEG ESEM fitted with an Oxford Instruments X-Sight EDS ATW X-Ray detector. Please see supplementary data 'F' for full methodology.

3. Results and discussion

3.1 Factors influencing the mobilisation of dissolved Pb

A key objective of the current study was to determine whether mining contaminated sediments became a source of dissolved Pb in response to flooding and draining sequences. The results indicated that these perturbations did influence the mobilisation of dissolved Pb, although patterns in the release of dissolved Pb were found to vary depending on the flood/drain sequence and the location (top/bottom) within the mesocosms.

The average concentration of dissolved Pb released over a flood period was significantly higher at the top of the mesocosm compared to the bottom ($z = -7.3$, $p = < 0.001$), ($z = - 2.525$, $p = < 0.05$), 1st and 2nd mesocosm experiments respectively. At the top of the mesocosm, within surface water, the concentraton of dissolved Pb increased over the duration of the flood. All variable wet and dry runs displayed significantly higher concentrations of dissolved Pb at the end of a flood compared to the start ($z = < -1.96$, $p = < 0.05$) (Figs 3a and 3b). In contrast, at the bottom of the mesocosm almost all of the dissolved Pb was released at the start of a flood (within 2-3 hours) and concentrations remained relatively constant, or declined over the flood period. There was no significant increase in dissolved Pb between the start and end of a flood period at the bottom of the mesocosm for the 2wdry, 3wdry, 2wwet and F/C runs ($z = > -1.96$, $p = > 0.05$), nor for the constant flood runs at the top ($z = -0.73$, $p = .465$) ($z = -1.424$, $p = 0.155$) and bottom ($z = -0.63$, $p = .53$) ($z = -0.316$, $p = 0.752$) of the 1st and 2nd mesocosm experiments respectively (Figs 3a and 3b). Similarities in the patterns of dissoved Pb release were apparent between the two mesocosm experiments possibly indicating the key geochemical mechanisms controlling Pb mobilisation were the same.

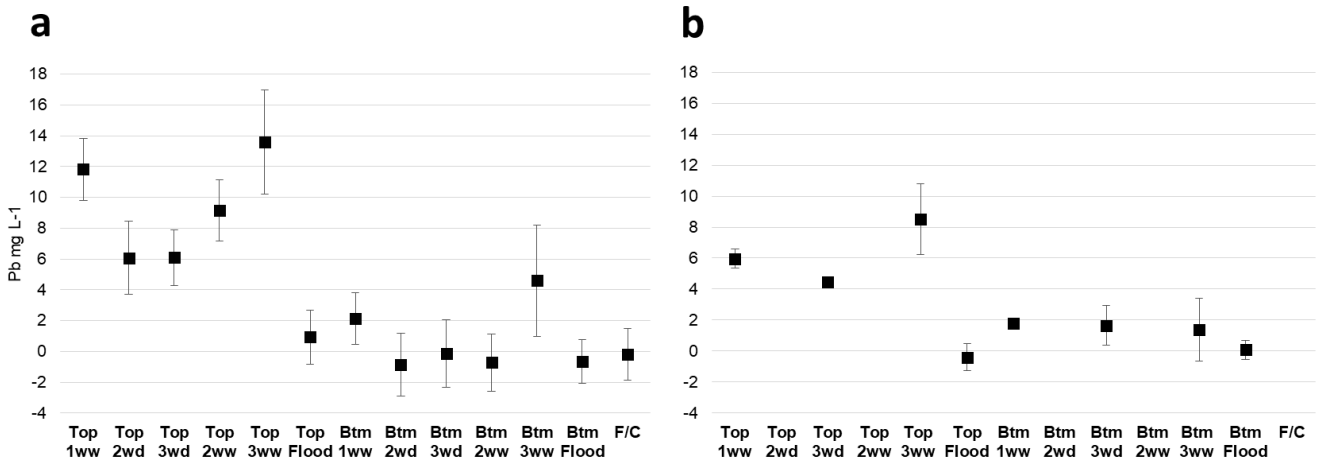

Fig. 3. Average concentration of dissolved Pb released over a flood period (mg L^{-1}) (concentration at the end of a flood minus concentration at the start) for all runs, top and bottom of the mesocosm for (a) 1st mesocosm experiment, bars indicate standard error (n=9 for 3wwet and 3wd, n = 12 for 2ww and 2wd, n = 18 for 1ww, flood and F/C) (b) 2nd mesocosm experiment bars indicate standard error (n=3 for 3wwet and 3wd, n = 5 for 1ww, flood).Principal components analysis was conducted on 8 items with orthogonal rotation (varimax) to determine the underlying factors influencing the mobilisation of Pb. Two PCs had eigenvalues greater than '1': PC1 explained 62.7% and PC2 explained 14.9% of the variance. PC1 showed a high positive loading for sulphate (0.958) and Ca (0.897) and a negative loading for Pb (-0.527). At the bottom of the mesocosms, runs with longer flood periods, particularly the constant flood run, scored highly against this component (Fig. 4). Pore and surface water chemical analysis found that average concentrations of dissolved sulphate and Ca were higher at the bottom of the mesocosms compared to the top (Tables 2 and 3) and correlation analysis for the flood run at the bottom of the mesocosm showed a significant negative relationship between Pb and sulphate ($r = -.889$, $p = <.01$) and Pb and Ca ($r = -.605$, $p = <.01$). These results could indicate that underlying factors contributing to the release of sulphate and Ca over flooded periods may be linked to the lower concentrations of Pb at the bottom of the mesocosms. Inorganic carbon (IC) in the sediment was below detection in the current study both prior to treatment and at the end of the run. Pore and surface water analysis indicted that bicarbonate concentrations were undetectable. Furthermore, it can be seen, section 3.2, Table 4, geochemical modelling, that no carbonate minerals were predicted to precipitate. Therefore it is unlikely the substitution of Ca for Pb in carbonate minerals such as calcite ($CaCO_3$), aragonite ($CaMg(CO_3)_2$, and ankerite ($Ca(Fe,Mg)CO_3)_2$ (Cravotta 2008; Fairchild et al. 2010) or the precipitation of Pb carbonate minerals

358 such as cerussite (VanLoon and Duffy, 2011) were key geochemical mechanisms controlling the
359 mobilisation of dissolved Pb. Sulphate was present at higher concentrations than the other anions
360 (nitrate, chloride and phosphate). In waters with high sulphate concentrations the production of
361 hydrogen sulphide and precipitation of insoluble metal sulphide galena (PbS) can serve as a sink for
362 dissolved Pb (Du Laing et al. 2009). However, although redox potential measurements were lower at
363 the bottom of the mesocosms than at the top (Table 3), they did not decline low enough for the
364 production of hydrogen sulphide (<120 mV) (Ross 1989; Gambrell et al. 1991; Bartlett 1999). Gypsum
365 ($CaSO_4.2H_2O$) is often present in mining impacted catchments (Younger, 1998; Harris et al., 2003;
366 Kuechler et al., 2004). Piper analysis indicated that the water samples were Ca-sulphate water type -
367 typical of mine drainage. Dissolution of this mineral could account for the presence of sulphate and
368 Ca in pore water and processes relating to the dissolution of this mineral could be linked to the
369 attenuation of dissolved Pb. This is discussed further in section 3.2.

370 High negative loadings for DO (-0.814) and redox potential (-0.942) were recorded against PC1 and
371 2. This is in line with the negative loading for Pb (-0.527) against PC1. Runs, at the top of the
372 mesocosms, scored negatively against PC1 and in some cases PC2 (3wwet run) (Fig.4). DO and
373 redox potential measurements showed conditions were oxic ~99.5% DO, Eh 494 mV at the top of the
374 mesocosms (Table 3). These results indicate that underlying factors linked to high DO and redox
375 potential conditions, may have contributed to releases of dissolved Pb over flood periods at the top of
376 the mesocosms. Correlation analysis for the 3wwet run indicated a significant positive relationship
377 between dissolved Pb and sulphate ($r = .605$, $p = <.01$) and dissolved Pb and Ca ($r = .828$, $p = <.01$).
378 The oxidation of Pb sulphide minerals such as galena in mine tailings and contaminated sediment has
379 been linked to the release of high concentrations of dissolved Pb into surface water during laboratory
380 inundation experiments (Wragg and Palumbo-Roe 2011) and in the field, in response to storm events
381 (Byrne et al 2012). The oxidation of galena would not necessarily produce excess acidity however,
382 any subsequent hydrolysis (Younger 1998) or adsorption reaction (Dzombak and Morel 1987) would
383 result in proton release. Therefore, the slightly acidic pH observed (pH 5.3, range 4.8 – 5.8), (pH 5.7,
384 range 5.1 – 5.8) during the 1st and 2nd mesocosm experiments respectively could be linked to these
385 acid producing processes and the poor buffering capacity of the water.

386

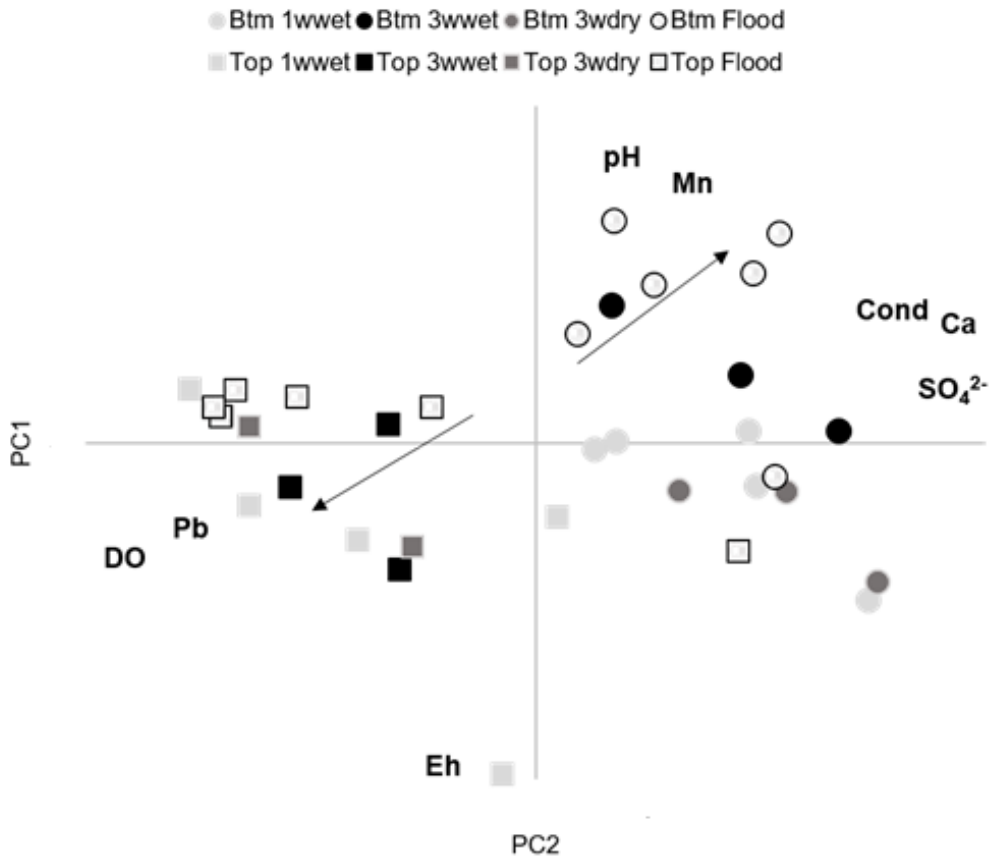

Fig. 4. Principal component analysis showing the distribution of pore water chemical samples along the first two principal components includes runs 1wwet, 3wwet, 3wdry, flood at the top (squares) and bottom (circles) of the mesocosms. Arrows indicate general trend for longer flooded runs (bottom) compared to 1wwet and 3wwet runs (top) (2^{nd} mesocosm experiment).

Table 2: 1st mesocosm experiment, Mean and range (in parenthesis) of dissolved (<0.45µm) metals and anions (mg l^{-1}), pH, Conductivity (µS/cm), Temperature (˚C) at the end of a flood, by run, Top (T) and Bottom (B) of the mesocosm, key average values (bold and underlined), n=#[1]

Run	1wwet (T)	1wwet (B)	2wdry (T)	2wdry (B)	3wdry (T)	3wdry (B)	2wwet (T)	2wwet (B)	3wwet (T)	3wwet (B)	Flood (T)	Flood (B)	F/C (B)
Location	**n=18**	**n=18**	**n=12**	**n=12**	**n=9**	**n=9**	**n=12**	**n=12**	**n=9**	**n=9**	**n=33**	**n=33**	**n=33**
pH	5.2	5.3	5.1	5.2	5.1	5.2	5.1	5.3	5.2	5.4	5.3	5.5	5.2
(Range)	(5 - 5.6)	(5.1 - 5.5)	(5 - 5.3)	(5.1 - 5.5)	(4.8 - 5.3)	(5 - 5.3)	(4.9 - 5.4)	(5.1 - 5.5)	(4.9 - 5.7)	(5.2 – 5.7)	(5 - 5.8)	(5 – 5.7)	(5.1 - 5.4)
Temp	22.3	23.1	22.3	23.0	23.0	23.8	22.6	23.3	22.0	22.7	22.4	23.1	22.9
(Range)	(20.9 - 24.2)	(21.9 - 24.8)	(21.2 - 23.3)	(21.7 - 23.9)	(21.4 - 24.4)	(22.3 - 25.1)	(20.4 - 24.5)	(20.9 - 25.1)	(21.4 - 22.6)	(22.1 - 23.2)	(19.9 - 24.5)	(29.9 - 25)	(21 - 25)
Cond	110.6	183.2	100.2	188.4	110.9	208.3	134.2	208.1	156.4	230.4	105.8	248.6	77.9
(Range)	(87 - 144)	(155 - 204)	(88 - 116)	(152 - 214)	(94 - 136)	(164 - 250)	(107 - 156)	(188 - 224)	(146 - 169)	(218 - 264)	(46 - 126)	(140 - 339)	(50 - 130)
Fe	0.0	0.4	0.0	0.6	0.0	0.2	0.0	3.0	0.0	6.0	0.0	8.9	0.0
(Range)	0.0	(0 - 1.7)	0.0	(0 - 1.6)	0.0	(0 - 0.8)	0.0	(2.2 - 3.9)	0.0	(3.6 - 10)	0.0	(0 - 27.7)	(0 - 0.5)
Mn	0.2	1.6	0.2	1.6	0.2	1.4	0.3	5.3	1.5	7.7	0.5	9.6	0.4
(Range)	(0.1 - 0.4)	(1.2 - 1.8)	(0.1 - 0.2)	(1.1 - 2.2)	(0.1 - 0.3)	(0.6 - 2.9)	(0 - 0.7)	(3.5 - 6.4)	(0.7 - 3.1)	(6.7 - 9.6)	(0 - 1.3)	(0.4 - 16.6)	(0 - 1)
Pb	17.1	14.1	15.4	13.9	14.3	12.6	18.5	13.2	**21.5**	14.4	17.2	**10.8**	10.2
(Range)	(9.8 - 22.3)	(8.6 - 24.3)	(13.2 - 17.2)	(12.5 - 15.2)	(10.8 - 16.8)	(10.6 - 16.1)	(14.7 - 24.4)	(10.1 - 13.2)	(16.7 - 30.6)	(9.7 - 24.7)	(5.2 - 27.2)	(3.9 - 28.5)	(4.2 - 23.7)
Ca	2.4	3.9	1.7	3.4	2.1	4.1	2.3	3.9	3.3	4.2	2.6	4.5	1.9
(Range)	(1.7 - 3.4)	(2.6 - 5)	(1.4 - 2.1)	(2.1 - 4.5)	(1.9 - 2.9)	(2.7 - 5.9)	(1.6 - 2.6)	(2.6 - 5)	(2.8 - 3.8)	(3.9 - 4.7)	(1.5 - 3.6)	(2.8 - 6.8)	(1.3 - 2.8)
NO_3^-	2.3	0.5	3.3	2.6	4.1	2.5	1.9	0.0	1.5	0.0	1.4	0.6	2.3
(Range)	(0 - 5.7)	(0 - 1.5)	(2 - 4.9)	(0 - 4.8)	(2.6 - 5.7)	(0 - 6)	(0.9 - 3)	0.0	(0 - 3.2)	0.0	(0 - 4.2)	(0 - 8.7)	(0.7 - 4.2)
Cl-	1.5	1.2	1.5	1.3	2.3	1.9	2.0	1.3	2.0	1.3	2.0	2.0	1.8
(Range)	(0.3 - 2.9)	(0 - 2.5)	(0.9 - 2.8)	(0.8 - 2.4)	(1.6 - 3.2)	(1.3 - 2.7)	(0.9 - 3.1)	(0.5 - 2.2)	(0.9 - 2.5)	(0.7 - 1.9)	(1.1 - 3)	(0.8 - 3.9)	(0 - 17.8)
SO_4^2	38.9	71.2	44.5	84.1	42.7	87.9	48.6	82.9	61.8	95.0	46.5	119.7	36.2
(Range)	(10.8 - 65)	(60.2 - 100.8)	(25.3 - 90.9)	(57.3 - 142.8)	(25.4 - 63.3)	(61.2-129.5)	(34.7 - 63.4)	(65.3 - 94.2)	(47.2 - 85)	(79.6 - 121.2)	(13.5 - 106.4)	(47.6 - 277.7)	(16.9 - 90.5)

[1] Note: 'n' relates to number of samples taken at the end of a flood period. The 'n' varied between runs because certain runs had more flood periods than others over the treatment period. Includes replicates.

Table 3: 2nd mesocosm experiment, Mean and range (in parenthesis) of dissolved (<0.45µm) metals and anions (mg L^{-1}), pH, Conductivity (µS/cm), Temperature (˚C), DOC (mg L^{-1}), TIC (mg L^{-1}) at the end of a flood, by run, Top (T) and Bottom (B) of the mesocosm, key average values (bold and underlined), n= #[2]

	1wwet (T) n=5	1wwet (B) n=5	3wdry (T) n = 3	3wdry (B) n = 3	3wwet (T) n = 3	3wwet (B) n = 3	flood (T) n = 10	Flood (B) n = 10
pH	5.5	5.7	5.6	5.7	5.6	5.8	5.7	5.8
(range)	(5.1 - 5.7)	(5.6 - 5.8)	(5.5 - 5.7)	(5.6 - 5.7)	(5.4 - 5.7)	(5.7 - 5.8)	(5.4 - 5.8)	(5.6 - 5.8)
Temp	17.5	17.8	17.7	17.7	18.4	18.9	17.9	18.2
(range)	(16 - 20)	(16.4 - 20.1)	(16.2 - 20.3)	(16.3 - 20.3)	(17 - 19.6)	(17.5 - 20)	(16 - 20.3)	(16.5 - 20.3)
Cond	225.2	392	175.3333	382	230.6667	405	264.9	408.4
(range)	(148 - 373)	(336 - 435)	(170 - 186)	(338 - 415)	(206 - 276)	(359 - 436)	(162 - 416)	(342 - 452)
D.O. %	100	34	102	37	94	18	102	12
(range)	(78 - 109)	(10.4 - 43.2)	(99 - 105)	(13.1 - 52.7)	(80.5 - 101)	(8.3 - 28.1)	(98 - 111	(7.8 - 23)
Eh	509	482	499	491	483	428	485	423
(range)	(459 - 603)	(456.9 - 530)	(479 - 525)	(478.9 - 509)	(468 - 504)	(412.7 - 436)	(446 - 555)	(381 - 485)
Fe	0.0	0.1	0.0	0.1	0.7	0.1	0.0	0.3
(range)	0.0	(0 - 0.1)	(0 - 0.1)	(0 - 0.2)	(0 - 2)	(0.1 - 0.2)	(0 - 0.2)	(0.1 - 0.6)
Mn	0.1	0.1	0.0	0.1	0.1	3.5	0.2	5.8
(range)	(0 - 0.1)	(0.1 - 0.2)	0.0	(0 - 0.2)	(0 - 0.1)	(2.2 - 5.3)	(0 - 0.7)	(1 - 10.1)
Pb	**8.3**	4.9	6.1	5.8	**10.0**	4.9	**8.6**	**3.8**
(range)	(8 - 9.2)	(3.8 - 5.6)	(5 - 6.7)	(4.3 - 7)	(7.5 - 14.2)	(2.3 - 6.9)	(5 - 15)	(1.7 - 4.8)
Ca	2.4	11.8	2.0	13.7	4.7	15.7	5.7	13.6
(range)	(0 - 8)	(8 - 14)	(0 - 4)	(16 - 12)	(3 - 7)	(14 - 17)	(0 - 18)	(4 - 19)
Nitrate	1.6	1.4	0.6	1.9	1.1	0.1	0.7	0.0
(range)	(0.2 - 2.8)	(0.6 - 2.3)	(0 - 1.2)	(1 - 2.5)	(0.4 - 1.7)	(0 - 0.2)	(0 – 2.1)	(0 - 0.5)
Chloride	8.5	3.3	1.7	2.6	4.0	3.5	7.8	6.0
(range)	(2.4 - 23.5)	(2.6 - 4.8)	(1.27 - 2.48)	(1.4 - 3.4)	(1.6 - 6.4)	(1.1 - 5.5)	(1.5 - 27.6)	(0.7 - 17.5)
Sulphate	25.3	95.2	17.7	120.3	36.0	110.3	35.5	94.6
(range)	(8.5 - 64)	(121.9 - 47.7)	(8.8 - 35.2)	(90 - 145)	(19.3 - 52.9)	(66.6 - 147.7)	(7 - 115)	(46 - 138)
Na	2.2	4.8	3.0	4.7	5.3	14.3	7.3	8.8
(range)	(0 - 4)	(3 - 7)	(1 - 6)	(3 - 7)	(4 - 7)	(9 - 19)	(1 - 22)	(2 - 18)
K	1.2	1.0	0.0	0.7	0.3	1.0	2.8	0.7
(range)	(0 - 4)	1.0	0.0	(0 - 1)	(0 - 1)	1.0	(0 - 25)	(0 - 1)
DOC	2.5	3.1	1.9	3.1	2.6	4.3	2.6	3.6
(range)	(2.1 - 3.2)	(2.4 - 3.5)	(1.9 - 2)	(2.6 - 3.8)	(1.9 - 3)	(3.7 - 4.9)	(1.9 - 4.9)	(2.5 - 4.8)
TIC	0.8	1.2	0.6	1.1	0.8	2.8	0.7	2.5
(range)	(0.4 - 1.1)	(0.6 - 1.8)	(0.3 - 0.9)	(0.7 - 1.6)	(0.7 - 1.1)	(2.3 - 3.4)	(0.2 - 1.4)	(1.1 - 4.3)

[2] Note: 'n' relates to number of samples taken at the end of a flood period. The 'n' varied between runs because certain runs had more flood periods than others over the treatment period.

400 **3.2 Solubility control of dissolved Pb concentrations in pore and surface water by equilibrium**
401 **with anglesite**

402 Anglesite has been reported to form as a weathering product from the oxidation of galena in mine
403 drainage environments (Harris et al. 2003; Palumbo-Roe et al 2013). To assess how close to
404 saturation the flood water solutions were with respect to mineral phases, particularly anglesite, that
405 may have formed over the treatment period, saturation indices (SI) were calculated using PHREEQC
406 (Ball and Nordstrom, 1991).

407 The three week wet run (top) and flood run (bottom) were selected for analysis because the highest
408 average concentration of dissolved Pb was observed for the 3wwet run at the top of the mesocosm
409 (21.5 $\pm$ 2.9 mg l^{-1}), (10 $\pm$ 2.1 mg l^{-1}) and the lowest average concentration was observed for the
410 constant flood run at the bottom (10.8 $\pm$ 2 mg l^{-1}), (3.8 $\pm$ 0.3 mg l^{-1}) (Tables 2 and 3). Mineral phases
411 and SI's were calculated from input data (Table A1) and are listed (Table 4).

412 **Table 4. Mineral Phases, SI and charge balance (%) (first mesocosm run)**

Week	D	H	L	D	H	L
Sample	3wwet	3wwet	3wwet	Flood	Flood	Flood
Location	Top	Top	Top	Bottom	Bottom	Bottom
Charge balance %	0.5	-0.8	-0.2	0.2	0	-0.1
Anglesite $PbSO_4$	**0.36**	**0.25**	**0.32**	**0.37**	**0.04**	**-0.07**
Larnakite $PbO:PbSO_4$	-1.58	-1.13	-1.52	-0.62	-1.41	-0.34
$Pb(OH)_2$	-2.09	-2.05	-2.54	-1.65	-2.12	-1.95
Gypsum $CaSO4.2H_2O$	-2.96	-3.02	-2.88	-2.72	-2.56	-2.46
Zincite ZnO	-4.94	-4.58	-5.06	-4.2	-4.12	-3.9
ZnO(a)	-4.96	-4.61	-5.03	-4.26	-4.2	-3.93
Bianchite $ZnSO_4:6H_2O$	-5.49	-5.28	-5.18	-5.18	-4.98	-5.02
ZnSO4:H2O	-6.76	-6.54	-6.47	-6.43	-6.22	-6.28
Melanterite $FeSO_4:7H_2O$	ND	ND	ND	-5.15	-4.63	-4.44
Pyrochroite $Mn(OH)_2$	-9.89	-9.42	-9.77	-8.41	-8.17	-7.77
Birnessite MnO_2	-20.09	-19.43	-20.17	-18.02	-17.77	-16.97

413 Note: All solution output results were checked for charge balance (within 5%). Small concentrations of Na were added to make
414 up for any charge imbalance. Na was not measured in the pore water, however concentrations measured in previous studies at
415 the sample site (Montserrat, 2010) were similar to the concentrations used to balance charges (7.5 – 32 mg/L). ND= no data/
416 dissolved Fe was below detection.

For both the 3 week wet (top) and constant flood (bottom) runs, surface and pore water conditions reached supersaturation with respect to anglesite by the end of the first 3 week flood (week D) (Table 4). For the constant flood run, pore water conditions then changed from supersaturated to saturated by weeks H and L. This was not the case for the 3 week wet run where conditions remained supersaturated over the entire treatment period.

The flood run, unlike the variable runs, was not periodically drained and exposed to atmospheric conditions. The sediment, to a large extent, remained saturated and the water stagnant so it is possible that this system could have moved towards an equilibrium state.

To test that theory, a simple script was run using PHREEQC to calculate the anglesite precipitation that would occur if the input data (Table A1) for sample weeks D, H, L reached saturation with respect to anglesite. The program also calculated the concentration of dissolved Pb that would be expected in pore water under these new saturated conditions (Fig 5). The script was run for both the flood run (btm) and 3wwet run (top) for comparison.

In theory, if pore water conditions reach supersaturation with respect to anglesite, as was found to occur for the 3 week wet and constant flood run (week D), according to Le Châtelier's principle anglesite precipitation would occur and result in the decline in dissolved Pb and sulphate concentrations.

$$\text{Log\_k } 10^{-7.79} = [PbSO_4^{2-}]_{(s)} \rightleftharpoons [Pb]_{(aq)}\,[SO_4^{2-}]_{(aq)}$$

For the flood run, week D, conditions were supersaturated with respect to anglesite (Table 4). Actual concentrations of Pb were higher in pore water than the concentrations predicted at equilibrium with respect to anglesite (Fig 5). By week L pore water conditions were no longer supersaturated (Table 4) and actual Pb concentrations had declined to 5mg/L (Fig 5). Predicted Pb concentrations at equilibrium for the flood run, weeks H and L were similar to actual Pb concentrations for these weeks (Fig 5), indicating that conditions had moved towards an equilibrium state.

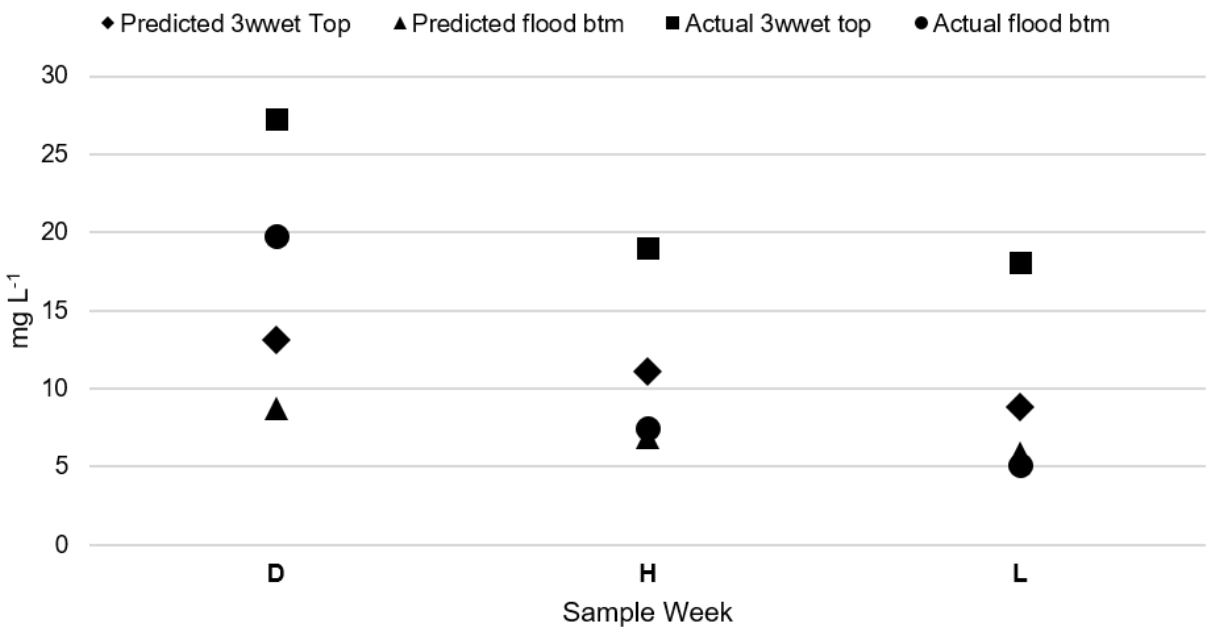

443

444 Fig 5. Concentrations of dissolved Pb measured (actual) in pore and surface water and calculated
445 (predicted) by bringing the system to saturation with respect to anglesite for the 3wwet (top) and flood
446 run (bottom) of the mesocosms (1st mesocosm experiment).

447 Predicted Pb concentrations for the 3wwet run at the top of the mesocosm were lower than actual Pb
448 concentrations (Fig 5). For this run, conditions reached supersaturation at the end of a three week
449 flood and anglesite precipitation was predicted to occur but the actual Pb concentration data shows
450 that this process did not result in a decline in dissolved Pb concentrations. The results indicate that
451 the system was not in equilibrium and the solubility of anglesite had little control over dissolved Pb
452 concentrations at the top of the mesocosms. For the 3wwet run long flood periods were followed by
453 short drainage periods and re-flooded though addition of fresh artificial rain water. Sediment would
454 therefore have been exposed to oxic conditions (particularly at the surface) that would have
455 encouraged oxidation of Pb sulphide minerals and release of dissolved Pb during periods of
456 innundation.

457 Concentrations of dissolved Pb were observed to be lower in the second mesocosm experiment
458 however saturation indices calculated for the 2nd mesocosm experiment using information from input
459 Table A2 showed that conditions at the bottom of the mesocosm were saturated with respect to
460 anglesite (Table B1). The high concentration of sulphate measured at the bottom of the mesocosms
461 during this experiment (Table 3) would have influenced saturation indices for anglesite. The
462 dissolution of sulphate bearing minerals such as gypsum may have contributed to the high sulphate

concentrations at the bottom of the mesocosms. SI calculations indicated gypsum was undersaturated, conditions that would favour the dissolution of this mineral. Batch-type experiments investigating the interaction of gypsum with Pb in aqueous solutions observed the rapid dissolution of gypsum and simultaneous formation of anglesite on the gypsum surface and in solution (Astillerox et al. 2010). In the current study sulphate producing mechanisms such as dissolution of soluble sulphates would have encouraged the rapid precipitaion of anglesite and provided a solubility control over dissolved Pb concentrations at the bottom of the mesocosm. Conditions were just below saturation with respect to anglesite at the top of the mesocosm (Table B1) and therefore it is likely the solubility of anglesite had little control over dissolved Pb concentrations at the top of the mesocosms for the 2nd mesocosm run.

3.3 Sediment analysis

Fe and Mn minerals have been reported as volumetrically the most important contaminant hosts in metal mining contaminated sediment in England and Wales (Hudson-Edwards 2003). Reactive 'easily reducible' Fe and Mn (hydr)oxides have been found to reduce more quickly (Lovley and Phillips 1987) at a higher redox potential (Du Laing et al. 2009) than older more crystalline forms such as goethite or hematite. Many studies have observed the partitioning of Pb with Fe and Mn hydroxides in metal contaminated sediments (Macklin and Dowsett 1989; Evans 1991; Hudson-Edwards 2003; Burton et al. 2005; Byrne et al. 2010; Farnsworth and Herring 2011). Dynamic changes in redox potential conditions and pH can bring about the reductive dissolution and precipitation of Fe and Mn hydroxides (Lovley and Philips 1986; Lee et al. 2002) and that can control the mobilisation of Pb (Charlatchka and Cambier 2000; Lesven et al. 2010).

Extraction step 1 was intended to remove reduced Fe, Mn and Pb loosely sorbed to the sediment surface and extraction step 2 was expected to recover easily reducible Fe and Mn (hydr)oxides along with any partitioned Pb. The first two extractions therefore represented the most labile forms of Fe and Mn. A control standard of ferrihydrite was synthesised using Poulton and Cranfield (2005) methodology and showed a 77% Fe recovery during extraction step 1. It is therefore likely that high concentrations of 'easily reducible' Fe were extracted during step 1. However, it can be seen from the results (Table 5) that relatively small concentrations of Fe and Mn were extracted from the sediment during the 1st and 2nd extractions compared to Pb. Almost all of the Pb (> 90%) was extracted during

492 the first 2 extraction steps (Fig. 6). The first extraction step was originally carried out on tidal river
493 surface sediment (Lovley and Phillips 1986). Sediment was not severely Pb-contaminated and
494 sulphate concentrations were in some cases an order of magnitude lower compared to the current
495 study. Although chemical extractions are intended to be phase specific total specificity is highly
496 unlikely (Leinz et al. 2000; Linge, 2008). Baba et al. (2011) reported that a 0.5 M HCl extraction
497 resulted in 30% Pb removal from an anglesite sample (< 63 µm) within 1 hour. Leinz et al. (2000)
498 carried out a series of Tessier et al. (1979) extractions and reported a 60,000 mg/kg recovery of Pb
499 from anglesite using an extraction of 0.25 M hydroxylamine hydrochloride in 0.25 M HCl for 30
500 mintues at 50ºC. Furthermore, 0.5 M HCl produces a low pH extraction and galena dissolution has
501 been found to increase as pH declines (Cama et al. 2005). It is possible therefore the high
502 concentration of Pb released during the 1st and 2nd extraction may be due, in part, to the presence of
503 other minerals, such as galena or anglesite in the sediment. The presence of these minerals was
504 corroborated through SEM/EDX analysis (Figs 8-10, Table 6.).

505 **Table 5 Mean concentrations (mg kg^{-1}) of metals in sediment (< 63 µm grain size) collected in**
506 **2012 and 2014 (n=3). Results are shown for pseudo-total metals and each geochemical phase**
507 **of the sequential extration.**

	Pb (2012)	Pb (2014)	Fe (2012)	Fe (2014)	Mn (2012)	Mn 2014)
Loosely sorbed	59,463.9 ±8589.6	59,807.2 ±2015.1	2,905.4 ±242.3	4,721.7 ±49.2	146.9 ±13.5	361.3 ±2.3
Easily reducible	25,306.4 ±3940.23	16,276.9 ±911.9	1,183.8 ±76.7	1,255.5 ±111.3	59.9 ±9.2	105.5 ±10.8
Reducible	0	0	22,973.3 ±1596.4	13,812.6 ±248.1	68.8 ±3.6	64.5 ±0.8
Residual	2952.9 ±1436.2	0	19,260.6 ±1452.8	24,078.5 ±990.6	330.9 ±24.2	386.4 ±15.1
Pseudo total	87,723.2	76,084.1	46,323.1	43,868.3	606.4	917.7
EA PEL guidelines *	91.3	91.3				

508

509 In the current study concentrations of dissolved Fe were very low in surface and pore water compared
510 to other metals (Table 2 and 3). Gotoh and Patrick (1974) found that under flooded conditions Fe

(hydr)oxide reductive dissolution occurred at 300 mV (pH 5), therefore this mechanism was unlikely to occur in the present study as redox potential measurements did not decline low enough, even at the bottom of the mesocosms. Furthermore microbial depletion of oxygen is limited by the availability of labile organic carbon (Gambrell et al. 1991) and the low-medium organic carbon measured in the current study would be unlikely to favour a large fall in redox potential conditions. The results of sediment and water analysis indicate that it is unlikely co-precipitation of Pb with Fe and Mn (hydr)oxides followed by reductive dissolution would have been a key mechanism controlling the mobilisation of Pb.

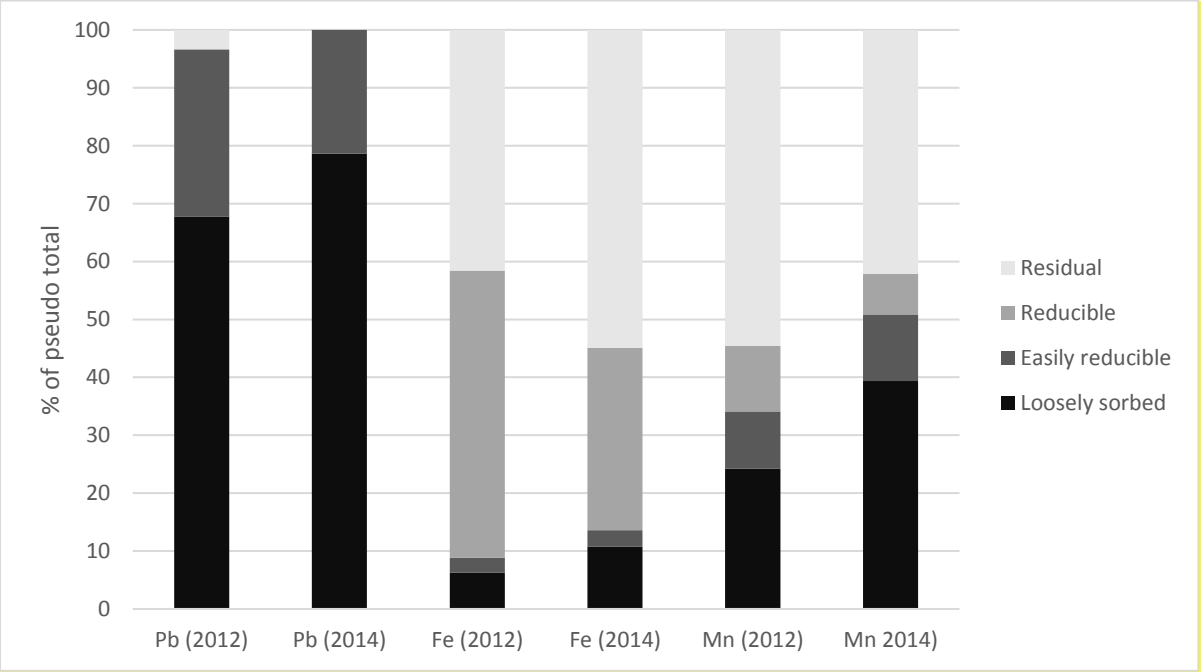

Fig 6. Mean sequential extraction and residual Pb, Fe and Mn concentrations (*n* = 3) in the sediment (< 63 µm grain size) collected in 2012 and 2014. Results are shown as percentages associated with each phase

Higher concentrations of Pb were found in the 'easily reducible' fraction of the sediment sampled during the 1st mesocosm run, compared to the 2nd (Table 5) and it is likely that differences in Pb concentration in the sediment were reflected in pore water concentrations (Fig. 7). The average concentration of 'dissolved' Pb was significantly lower for 2nd mesocosm experiment in 2014 compared to the 1st experiment in 2012 for all runs at the top and bottom of the mesocosm ($z = < -1.96$, $p = < 0.05$). Average concentrations were approximately 2 – 3 times lower (Fig. 7). Sediment collected in 2012 was taken from piles of mine tailings that had been dumped along the side of the river due to inefficient processes at the time of extraction. This waste would contain high

concentrations of the original ore minerals and their oxidised products. In 2014 sediment was collected from a different riverbank location closer to the river channel. This sediment may have been deposited during overbank flooding and as wash load transported from waste piles surrounding the site, this process has been described by (Merrington and Alloway 1994). The spatial heterogeneity of the post mining landscape is problematic with regards to predicting diffuse pollution. The above results highlight the importance of characterising the sediment within a catchment prior to modelling pollutant releases.

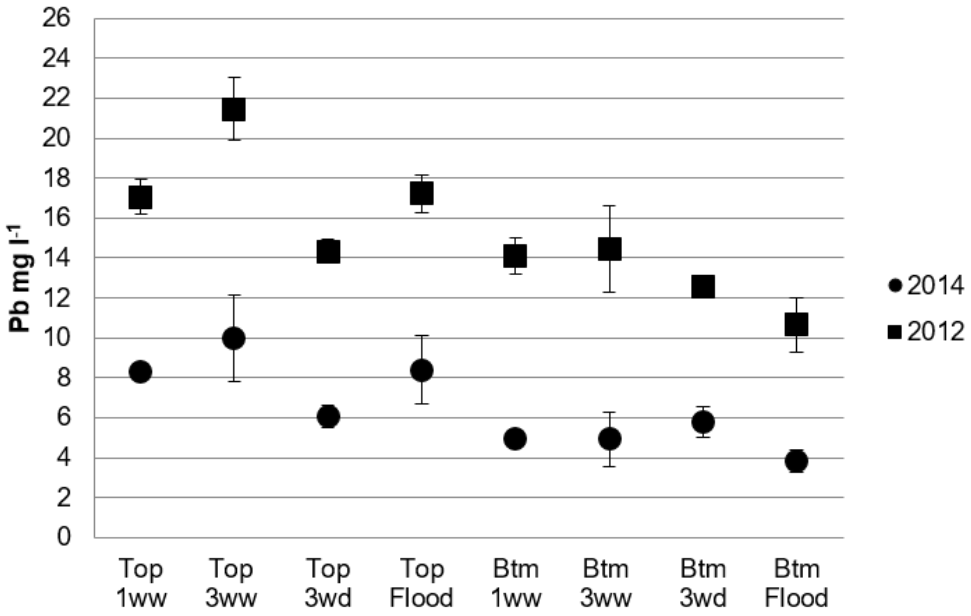

Fig 7. Average concentration (mg l^{-1}) of dissolved Pb released at the end of a flood for mesocosm experiments in 2012 and 2014 by run at the top and bottom. Bars indicate standard error 1st mesocosm experiment n=9 for 3wwet and 3wd, n = 12 for 2ww and 2wd, n = 18 for 1ww, flood and F/C; 2nd mesocosm experiment n=3 for 3wwet and 3wd, n = 5 for 1ww, flood.

SEM/EDX analysis was carried out to identify possible mineral associations of Pb in the sediment. Fig. 8 shows a back scattered electron image of the sediment (1st mesocosm run). Heavy elements (high atomic number) backscatter electrons more strongly than light elements (low atomic number) and therefore appear brighter in the image. As Pb is considered a heavier element, a bright grain was selected for analysis (spectrum 3) and a magnified back scattered electron image taken (Fig. 9).

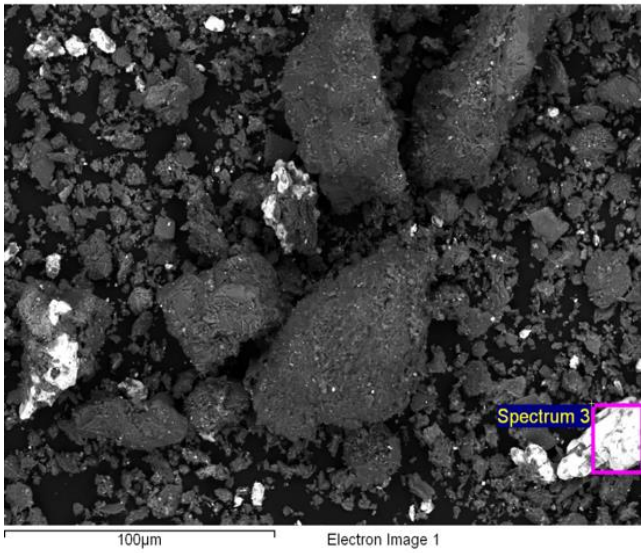

549

550 Fig. 8 Back scattered electron image of sediment (1st mesocosm run)

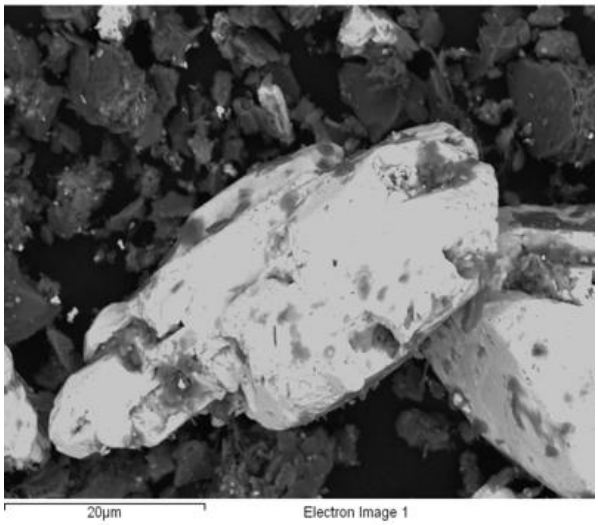

551

552 Fig. 9. Magnified Back scattered electron image of the grain in spectrum 3

553 EDX was carried out and the resulting quant specification (Table 6) shows an atomic % close to 1:1
554 ratio for Pb and S which could possibly indicate the presence of the mineral galena.

555 Table 6. Quant specification for spectrum 3

Element	Weight%	Atomic%

S K	13.13	**45.43**
Mn K	-0.07	-0.14
Fe K	2.85	5.65
Zn L	3.46	5.87
Pb M	80.64	**43.19**
Totals	100.00	

The smart map pattern (See supplementary data 'G') for elements Pb, S and Fe shows that the grain in spectrum 3 is likely to be a Pb, S mineral. A similar pattern of Pb and S was found throughout the sediment indicating this mineral was widely distributed. Fe did not show the same pattern and was not found to be partitioned with Pb. Mn was difficult to quantify through SEM/EDS, possibly due to lower total concentrations of this element in the sediment.

3.4 Conceptual model for dissolved Pb mobilisation

The results from the current study were used to create a simple conceptual model showing the key geochemical mechanisms controlling the release and attenuation of Pb. The model contrasts two key hydrological runs, the prolonged 3 wwet run with a short period of drainage and the constant flood (control) run. Both include a prolonged water residence time to allow reactions to occur at the sediment/water interface, however, the period of drainage for the 3 wwet run allows exposure to atmospheric conditions, particularly at the surface. These conditions would promote the oxidation of galena and result in the release of dissolved Pb into surface water upon re-wetting. In contrast, for the prolonged flood period with no period of drainage there would be little exposure to atmospheric conditions and oxygen, particularly deeper in the sediment. This would serve to reduce the rate of galena oxidation and conditions may 'stagnate'. High dissolved Pb concentrations and dissolution of sulphate bearing minerals such as gypsum may result in saturation with respect to anglesite leading to the attenuation of dissolved Pb. The 3wwet run is shown at the top of the mesocosm and the flood run at the bottom of mesocosm to highlight where the pattern of dissolved Pb mobilisation/ attenuation is most pronounced for each run. The dashed arrows indicate the depth at which key mechanisms have less of an influence on the pattern of dissolved Pb release.

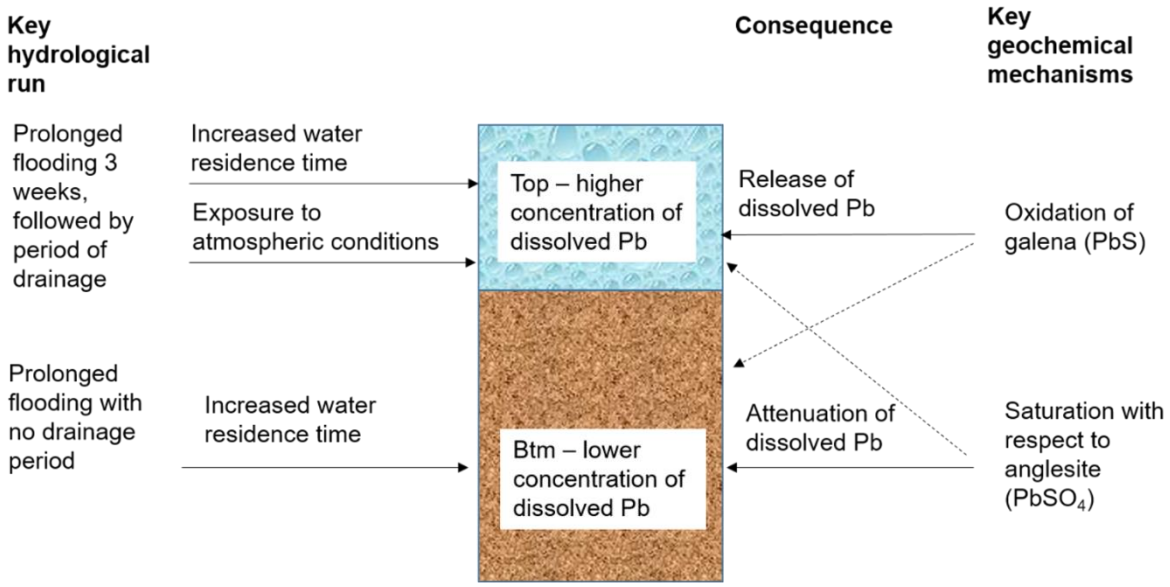

Simple conceptual model summarising the key hydrogeochemical mechanisms controlling the release and attenuation of Pb in response to 'riverbank' inundation and drainage

578

579 Fig. 11. Simple conceptual model showing the key geochemical mechanisms controlling the release
580 and attenuation of Pb.

581 The environmental factors controlling diffuse pollution from contaminated riverbank sediment are
582 currently seen as a 'black box' from a process perspective. The current study is the first to uncover
583 the key mechanisms responsible for dissolved Pb release into the riverine environment.

584 Compared to a previous study of Zn mobilisation in riverbank sediments (Lynch et al 2017), the
585 current research has found that the geochemical mechanisms controlling the release of dissolved Pb
586 are dissimilar. Due to different geochemical mechanisms controlling mobilisation for Pb and Zn, the
587 patterns of release were found to be different in response to the flood/ drainage runs. High
588 concentrations of dissolved Zn were released (i) immediately on flood wetting following a long dry
589 antecedent period, and (ii) in response to prolonged flooding, at the bottom of the mesocosm, due to
590 reductive dissolution processes. In the current study, the highest concentration of dissolved Pb
591 release was observed at the surface, in response to longer/ more frequent flood periods, with
592 intermittent drainage episodes that promoted oxic conditions. 3.5 Environmental risk of contaminated
593 sediments

594 Pb is listed as a priority substance in the Water Framework Directive 2013/39/EU, 12th August 2013,
595 amending directives 2000/60/EC and 2008/105/EC in the field of water policy. These directives note

that maximum allowable concentrations (MAC) should be taken into account in the river basin management plans covering period 2015 to 2021. For inland surface waters the annual average for Pb and its compounds is 1.2 µg l^{-1} (bioavailable). Where risk to, or via, the aquatic environment as a result of acute exposure has been identified, maximum allowable concentrations (MAC = 14 µg l^{-1}) have been applied. The EU standard takes into the account the influence of DOC on the toxicity of Pb but unlike the standard for Zn it does not require consideration of Ca. A metal bioavailability assessment tool has been developed for Pb that takes into consideration the influence of DOC. Using the highest concentrations of DOC 4.9 mg L^{-1} measured in the current study the calculated predicted no effect concentration (PNEC) of Pb (the calculated dissolved concentration of Pb that is equivalent to the EQSavailable for local water conditions at the site) is 5.88 µg L^{-1}.

Comparing the above standards to the results from dilution calculations (Table 7) it can be seen that dissolved Pb concentrations for all runs exceed MAC and PNEC and therefore would be expected to cause adverse environmental effects and pose a significant environmental risk.

Table 7.
Diluted Pb min and max average concentrations for 1st and 2nd mesocosm experiments

Mesocosm experiment #	Pb mg l^{-1}	Pb after dilution µg l^{-1}
1st experiment (max)	21.5	34.4
1st experiment (min)	10.8	17.28
2nd experiment (max)	10	16
2nd experiment (min)	3.8	6.08

There are currently no mandatory threshold values for trace metal contaminants in river sediments in the UK and Europe. This is due to (i) The challenges of setting fixed standards in river systems where contamination is spatially highly variable and (ii) limited toxicological data (Environment Agency, 2008). Catchments with a long history of mining are often naturally highly mineralised and difficulties can arise when assessing the precise environmental risk contaminated soils and sediment may pose (Dennis et al., 2003). There are however interim sediment quality guideline values developed by the Environment Agency (Environment Agency, 2008) that are used to trigger further investigation. Predicted effect level (PEL) is the level above which adverse biological effects are expected to occur. It can be seen that sediment sampled for the 1st and 2nd mesocosm experiments contained high

621 concentrations of Pb (Table 5). All samples far exceed predicted effect level (PEL) concentrations and
622 therefore could pose a significant environmental risk. It should be noted that these intermim standards
623 relate to in-channel sediments, rather than river bank sediments, but in the absence of other
624 standards relating to sediment they have been used as a guide.

625 PEL values relate to total metals (including residual forms) and therefore provide no indication of the
626 potential bioavailability of trace metal contaminants. A recent study of Pb contaminated soil found that
627 LC 50 values (concentration of Pb causing 50% mortality) for earth worms were far lower for acidic
628 soils, pH 4.96 (1161 mg Kg^{-1}) compared to neutral, pH 6.94 (4648 mg Kg^{-1}) or alkaline, pH 8.45 (7851
629 mg Kg^{-1}) soils and concluded that soil properties are important factors that modify bioavailability
630 (Wijayawardena et al. 2017). In the current study the low inorganic carbon concentrations of the
631 sediment indicate a slightly acidic environment that may favour increased bioavailability. Furthermore
632 all concentrations of Pb measured in the current study exceeded all LC 50 values regardless of pH.
633 The high concentration of Pb present in the most labile fractions of the sediment indicate that
634 dissolved Pb could easily be released into pore and surface water in response to environmental
635 perturbations with potentially serious adverse effects on water quality, aquatic flora and fauna and the
636 surrounding agricultural and grazing land (Walling et al. 2003; Foulds et al. 2014).

637 **4. Conclusions**

638 The Cwmystwyth mine has been identified as a top 30 priority mining 'impacted' waterbody in western
639 Wales river basin district (Environment Agency 2012b). Although mining has ceased at the site the
640 sediment remains severely Pb-contaminated. Results of the current study indicate the sediment is
641 likely to act as source of dissolved Pb pollution to the Afon Ystwyth. Historical studies have found high
642 concentrations of Pb (68 µg l^{-1}) in the river water half a km below the Cwmyswyth mine area with
643 concentrations remaining high (58 µg l^{-1}) up to 7.5 km downstream although more recent studies
644 found concentrations of dissolved Pb to be below detection (Montserrat 2010).

645 A previous mesocosm study by Lynch et al. (2017) found high concentrations of dissolved Zn may be
646 released from stream riverbanks over prolonged flood periods due to the reductive dissolution of Mn
647 (hydr)oxides. Pb is generally reported as less mobile than dissolved Zn. However, results from the
648 current study indicate that high concentrations of dissolved Pb could be released in response to

longer or more frequent flood events where periodic drainage events serve to keep conditions more oxic, particularly at the surface.

This is a concern because climate projections indicate a rise in the occurrence of localized heavy rainfall events, particularly in winter (DEFRA 2012b). Projected increases in flood events, particularly during winter months could result in a rise in river stage leading to prolonged inundation of river bank sediment and the mobilisation of dissolved Pb. Anglesite solubility may control dissolved Pb concentrations with depth, but have little control at the sediment surface where continual oxidation of galena and subsequent releases of dissolved Pb may occur. Where flood conditions subside a fall in river stage and exfiltration could result in a pulse of dissolved Pb released into river systems. Dilution calculations indicate that concentrations of dissolved Pb released are likely to exceed MAC in river water and therefore pose a significant environmental risk.

This study is unique in linking key hydrological processes that may occur due to climate change to hydrogeochemical mechanisms controlling dissolved Pb mobilisation. The mineralogy at the Cwmystwyth site is common to many mining impacted sites and it is likely that the mechanisms identified in the current study would be widespread in the UK and worldwide. As these pollution events are transient the 'exact sources' of Pb pollution would be difficult to identify in the field in the absence of continuous sampling methodologies. As a result Pb pollution events could go unnoticed. The authors suggest that further field studies are carried out that focus on understanding how stream-floodplain connectivity could drive diffuse Pb pollution at mining impacted sites particularly under variable hydrometeorological conditions.

Acknowledgements

This research was funded by NERC ID: NE/J500240/1

Conflicts of Interest

The authors declare no conflict of interest

673 **5. References**

674 Appelo CAJ, Postma D. Geochemistry, groundwater and pollution. Leiden, The Netherlands: A.A.
675 Balkema Publishers, 2010.

676 Astillerosa JM, Godelitsasb A, Rodríguez-Blancoc JD, Fernández-Díaza L, Prietod M, Lagoyannise A,
677 et al. Interaction of gypsum with lead in aqueous solutions. Appl. Geochem. 2010; 25: 1008-1016.

678 Baba AA, Adekola FA, Fapojuwo DPT, Otokhina FO. Dissolution kinetics and solvent extraction of
679 lead from anglesite ore. Journal of the Chemical Society of Nigeria 2011; 36: 157-164.

680 Bartlett RJ. Characterizing soil redox behaviour. In: Sparks DL, editor. Soil Physical Chemistry. CRC
681 Press, Boca Raton, FL., 1999, pp. 371-397.

682 Bick DE. The Old Metal Mines of Mid-Wales. Part 1 Cardiganshire - South of Devil's Bridge. Newent,
683 Glos.: The Pound House, 1976.

684 Bradley SB. Long-term Dispersal of Metals in Mineralised Catchment by Fluvial Processes. In: Foster
685 IDL, Gurnell AM, Webb BW, editors. Sediment and Water Quality in River Catchments John Wiley &
686 Sons Ltd, 1995, pp. 161-177.

687 British_Geological_Survey. British Regional Geology: Wales. Nottingham: British Geological Survey,
688 2007.

689 Buckby T, Black S, Coleman ML, Hodson ME. Fe-sulphate-rich evaporative mineral precipitates from
690 the Rio Tinto, southwest Spain. Mineral. Mag. 2003; 67: 263-278.

691 Buekers J, Amery F, Maes A, Smolders E. Long-term reactions of Ni, Zn and Cd with iron
692 oxyhydroxides depend on crystallinity and structure and on metal concentrations. Eur. J. Soil Sci.
693 2008; 59: 706-715.

694 Burton GA. Metal Bioavailability and Toxicity in Sediments. Crit. Rev. Environ. Sci. Technol. 2010; 40:
695 852-907.

696 Burton ED, Phillips IR, Hawker DW. Geochemical Partitioning of Copper, Lead and Zinc in Benthic,
697 Estuarine Sediment Profiles. J. Environ. Qual. 2005; 34: 263-273.

698 Byrne P, Reid I, Wood PJ. Stormflow hydrochemistry of a river draining an abandoned metal mine:
699 the Afon Twymyn, central Wales. Environ Monit Assess 2013; 185: 2817–2832.

700 Byrne P, Wood PJ, Reid I. The impairment of river systems by metal mine contamination: A review
701 including remediation options. Critical Reviews in Environmental Science and Technology. Crit. Rev.
702 Environ. Sci. Technol. 2012; 42: 2017-2077.

703 Byrne P, Reid I, Wood PJ. Sediment geochemistry of streams draining abandoned lead/zinc mines in
704 central Wales: the Afon Twymyn. Journal of Soils and Sediments 2010; 10: 683-697.

705 Caetano M, Madureira MJ, Vale C. Metal remobilisation during resuspension of anoxic contaminated
706 sediment: short-term laboratory study. Water, Air, and Soil Pollution 2003; 143: 23-40.

707 Cama J, Acero P, Ayora C, Lobo A. Galena surface reactivity at acidic pH and 25^{o}C based on flow-
708 through and in situ AFM experiments. Chemical Geology 2005; 214: 309-330.

709 Carroll SA, O'Day PA, Piechowski M. Rock-water interactions controlling zinc, cadmium, and lead
710 concentrations in surface waters and sediments, US Tri-State Mining District. 2. Geochemical
711 interpretation. Environ. Sci. Technol. 1998; 32: 956-965.

712 Centre for Ecology and Hydrology. National river flow archive. 2015. Accessed: 101015. Available
713 from: http://www.ceh.ac.uk/data/nrfa/data/station.html?63004

714 Charlatchka R, Cambier P. Influence of reducing conditions on solubility of trace metals in
715 contaminated soils. Water, Air, Soil Pollut. 2000; 118: 143-167.

716 Chibuike GU, Obiora SC. Heavy metal polluted soils: Effect on plants and bioremediation methods.
717 Appl. and Env. Soil Sci. 2014; 2014: 1-11.

718 Cid N, Ibanez C, Palanques A, Prat N. Patterns of metal bioaccumulation in two filter-feeding
719 macroinvertebrates: exposure distribution, inter-species differences and variability across
720 developmental stages. Sci. Total Environ. 2010; 408: 2795-806.

721 Ciszewski D and Grygar Tomas Matys. A review of flood-related storage and remobilisation of heavy
722 metal pollutants in river systems. Water, Air, & Soil Pollution 2016, 227 – 239.

723 Collins A, Ohandja D, Hoare D, Voulvoulis N. Implementing the Water Framework Directive: a
724 transition from established monitoring networks in England and Wales. Environmental Science &
725 Policy 2012; 17: 49-61.

726 Cravotta CA. Dissolved metals and associated constituents in abandoned coal-mine discharges,
727 Pennsylvania, USA. Part 2: Geochemical controls on constituent concentrations. Appl. Geochem.
728 2008; 23: 203-226.

729 DEFRA. Climate Change Risk Assessment for the water sector. Project Code GA0204. In: DEFRA,
730 editor. Crown, 2012a.

731 DEFRA. Climate Change Risk Assessment for the Floods and Coastal Erosion Sector Project code
732 GA0204, Wallingford, 2012b.

733 Dennis IA, Macklin MG, Coulthard TJ, Brewer PA. The impact of the October-November 2000 floods
734 on contaminant metal dispersal in the River Swale catchment, North Yorkshire, UK. Hydrological
735 Processes 2003; 17: 1641-1657.

736 Du Laing G, Rinklebe J, Vandecasteele B, Meers E, Tack FMG. Trace metal behaviour in estuarine
737 and riverine floodplain soils and sediments: A review. Sci. Total Environ. 2009; 407: 3972-3985.

738 Du Laing G, Vanthuyne DR, Vandecasteele B, Tack FM, Verloo MG. Influence of hydrological regime
739 on pore water metal concentrations in a contaminated sediment-derived soil. Environ. Pollut. 2007;
740 147: 615-625.

741 Dzombak DA, Morel FMM. Adsorption of inorganic pollutants in aquatic systems. Journal of Hydraulic
742 Engineering-Asce 1987; 113: 430-475.

743 Environment_Agency. Prioritisation of abandoned non-coal mine impacts on the environment.
744 SC030136/R2 The national Picture Environment Agency, 2012a.

745 Environment_Agency. Prioritisation of abandoned non-coal mine impacts on the environment.
746 SC030136/R6 The Western Wales River Basin District., 2012b.

747 Environment_Agency. Prioritisation of abandoned non-coal mine impacts on the environment project
748 summary SC030136/S14. Environment Agency, 2010.

749 Environment_Agency. Assessment of metal mining contaminated river sediments in England and
750 Wales. Environment Agency, Bristol, 2008.

751 Evans D. Chemical and physical partitioning in contaminated stream sediments in the River Ystwyth,
752 Mid-Wales. Environmental Geochemistry and Health 1991; 13: 84-92.

753 Fairchild IJ, Spotl C, Frisia S, Borsato A, Susini J, Wynn PM, et al. Petrology and geochemistry of
754 annually laminated stalagmites from an Alpine cave (Obir, Austria): seasonal cave physiology.
755 Geological Society, London, Special Publications 2010; 336: 295-321.

756 Farnsworth CE, Hering JG. Inorganic Geochemistry and Redox Dynamics in Bank Filtration Settings.
757 environmental science & technology 2011; 45: 5079-5087.

758 Foulds SA, Brewer PA, Macklin MG, Haresign W, Bretson RE, Rassner SME. Flood-related
759 contamination in catchments affected by historical metal mining: An unexpected and emerging hazard
760 of climate change. Sci. Total Environ. 2014: 476-477.

761 Fuge R, Laidlaw IMS, Perkins WT, Rogers KP. The influence of acidic mine and spoil drainage on
762 water quality in the mid-Wales area. Environmental Geochemistry and Health 1991; 13: 70-75.

763 Galan E, Gomex-Ariza JL, Gonzalez I, Gernandez-Caliani JC, Morales E, Giraldez I. Heavy metal
764 partitioning in river sediments severely polluted by acid mine drainage in the Iberian Pyrite Belt.
765 Applied Geochemistry 2003; 18: 409-421.

766 Gambrell., Delaune RD, Patrick JRW. Redox Processes in Soils following Oxygen Depletion. In:
767 Jackson MB, Davies, D.D., Lambers, H., editor. Plant Life Under Oxygen Depriviation. SPB Academic
768 Publishing, The Hague, 1991, pp. 101-117.

769 Gotoh S, Patrick WH. Transformation of iron in a waterlogged soil as influenced by redox potential
770 and pH. Soil Science Society of America Journal 1974; 38: 66-71.

771 Grundl T, Delwiche J. Kinetics of Ferric Oxyhydrixide precipitation. Journal of Contaminant Hydrology
772 1993; 14: 71-97.

773 Harris DL, Lottermoser BG, Duchesne J. Ephemeral acid mine drainage at the Montalbion silver mine,
774 north Queensland. Australian Journal of Earth Sciences 2003; 50: 797 - 809.

775 Hudson-Edwards KA. Sources, mineralogy, chemistry and fate of heavy metal-bearing particles in
776 mining-affected river systems. Mineral. Mag. 2003; 67: 205-217.

777 Hughes SJS. The Cwmystwyth Mines. Vol 17: Northern Mine Research Society, 1981.

778 Krause S, Hannah DM, Fleckenstein JH, Heppell CM, Kaeser D, Pickup R, et al. Inter-disciplinary
779 perspectives on processes in the hyporheic zone. Ecohydrology 2010; 4: 481-499.

780 Kuechler R, Klause N, Zorn T. Investigation of gypsum dissolution under saturated and unsaturated
781 water conditions. Ecological Modelling 2004; 176: 1-14.

782 Lee G, Bigham JM, Faure G. Removal of trace metals by coprecipitation with Fe, Al and Mn from
783 natural waters contaminated with acid mine drainage in the Ducktown Mining District, Tennessee.
784 Appl. Geochem. 2002; 17: 569-581.

785 Leinz RW, Sutley SJ, Desborough GA, Briggs PH. An Investigation of the Partitioning of Metals in
786 Mine Wastes Using Sequential Extractions. ICARD 2000: Proceedings from the Fifth International
787 Conference on Acid Rock Drainage 2. U.S. Geological Survey, Denver, Colorado, 2000.

788 Lesven L, Lourino-Cabana B, Billon G, Recourt P, Ouddane B, Mikkelsen O, et al. On metal
789 diagenesis in contaminated sediments of the Deule river (northern France). Appl. Geochem. 2010; 25:
790 1361-1373.

791 Linge KL. Methods for Investigating Trace Element Binding in Sediments. Critical Reviews in
792 Environmental Science & Technology 2008; 38: 165-196.

793 Lovley DR, Phillips EJP. Manganese inhibition of microbial iron reduction in anaerobic sediments.
794 Geomicrobiology Journal 1989; 6: 145-155.

795 Lovley DR, Phillips EJP. Competitive Mechanisms for Inhibition of Sulfate Reduction and Methane
796 Production in the Zone of Ferric Iron Reduction in Sediments. Appl. Environ. Microb. 1987; 53: 2636-
797 2641.

798 Lovley DR, Phillips EJP. Availability of Ferric Iron for Microbial Reduction in Bottom Sediments of the
799 Freshwater Tidal Potomac River. Appl Environ Microb. 1986; 52: 751-757.

800 Lynch SFL, Batty LC, Byrne P. Critical control of flooding and draining sequences on the
801 environmental risk of Zn-contaminated riverbank sediments. J. Soils Sediments 2017; 17: 2691-2707.

802 Lynch SFL, Batty LC, Byrne P. Environmental risk of metal mining contaminated river bank sediment
803 at redox-transitional zones. Minerals 2014; 4: 52-73.

804 Mayes WM, Potter HAB, Jarvis AP. Riverine Flux of Metals from Historically Mined Orefields in
805 England and Wales. Water, Air, Soil Pollut. 2013; 224: 1425.

806 Merrington G, Alloway BJ. The transfer and fate of Cd, Cu, Pb, and Zn from two historic metalliferous
807 mine sites in the U.K. Appl. Geochem. 1994; 9: 677-687.

808 MET Office. Climate. Met Office. 2016. Accessed: 170816. Available from:
809 http://www.metoffice.gov.uk/public/weather/climate/gcm3c7x2r.

810 Met Office (2017): UKCP09: Met Office regional land surface climate observations - long term
811 averages for administrative regions and river basins. Centre for Environmental Data Analysis.
812 Accessed: 050418. Available from:
813 http://catalogue.ceda.ac.uk/uuid/51132aea5ed0433ca338d32a912e3976

814 Montserrat AM. Environmental impact of mine drainage and its treatment on aquatic communities.
815 Water Sciences Group. PhD. University of Birmingham, 2010.

816 Macklin MG, Dowsett RB. The Chemical and Physical Speciation of Trace-Metals in fine-grained
817 overbank flood sediments in the Tyne basin, Northeast England. Catena 1989; 16: 135-151.

818 Natural Resources Wales. A Metal Mines Strategy for Wales. Natural Resources Wales, Wales, 2004.

819 Neal C, Reynolds B, Neal M, Pugh B, Hill L, Wickham H. Long-term changes in the water quality of
820 rainfall, cloud water and stream water for moorland, forested and clear-felled catchments at
821 Plynlimon, mid-Wales. Hydrology and Earth System Sciences 2001; 5: 459-476.

822 Nordstrom DK, Alpers CN. Geochemistry of Acid Mine Waters. In: Plumlee GSaL, M.J., editor. The
823 Environmental Geochemistry of Mineral Deposits. Part A: Processes, Techniques, and Health Issues.
824 6A. Society of Economic Geologists, Inc. , Colorado, USA, 1999, pp. 133-160.

825 Oxford Instruments. INCAEnergy Applications training notes. Bucks: Oxford Instruments, 2008.

826 Palumbo-Roe B, Wragg J, Cave M, Wagner D. Effect of weathering product assemblages on Pb
827 bioaccessibility in mine waste: implications for risk management. Environmental Science & Pollution
828 Research 2013; 20: 7699 - 7710.

829 Palumbo-Roe B, Wragg J, Banks VJ. Lead mobilisation in the hyporheic zone and river bank
830 sediments of a contaminated stream: contribution to diffuse pollution. J. Soils Sediments 2012; 12:
831 1633-1640.

832 Poulton SW, Canfield DE. Development of a sequential extraction procedure for iron: implications for
833 iron partitioning in continentally derived particulates. Chem. Geol. 2005; 214: 209-221.

834 Ross S. Soil Processes. New York: Routledge, 1989.

835 Shaheen SM, Rinklebe J, Rupp H, Meissner R. Temporal dynamics of pore water concentrations of
836 Cd, Co, Cu, Ni, and Zn and their controlling factors in a contaminated floodplain soil assessed by
837 undisturbed groundwater lysimeters. Environ Pol 2014; 191: 223-231.

838 Sharma P, Dubey RS. Lead toxicity in plants. Braz. J. Plant Physiol 2005; 17: 35-52.

839 Shimadzu Scientific Instruments. List of Shimadzu Application Notes, 2014.

840 Smith K. Metal sorption on mineral surfaces: an overview with examples relating to mineral deposits
841 vol 6A. The environmental geochemistry of mineral deposits part a: processes, techniques and health
842 issues. Society of Economic Geologists, Colorado, USA, 1999.

843 Stumm W, Sulzberger B. The Cycling of Iron in Natural Environments: considerations based on
844 labroatory studies of heterogeneous redox processes. Geochimica Et Cosmochimica Acta 1992; 56:
845 3233-3257.

846 Tessier A, Campbell PGC, Bisson M. Sequential Extraction Procedure for the speciation of particulate
847 trace metals. Analytical Chemistry 1979; 51: 844-851.

848 Torres E, Ayora C, Canovas CR, Garcia-Robledo E, Glalvan L, Sarmiento AM. Metal cycling during
849 sediment early diagenesis in a water reservoir affected by acid mine drainage. Sci. Total Environ.
850 2013; 461-462: 416-429.

851 Tripole S, Gonzalez P, Vallania A, Garbagnati M, Mallea M. Evaluation of the impact of acid mine
852 drainage on the chemistry and the macrobenthos in the Carolina Stream (San Luis-Argentina).
853 Environ. Monit. Assess. 2006; 114: 377-389.

854 Ullrich SM., Ramsey MH. Helios-Rybicka E. Total and exchangeable concentrations of heavy metals
855 in soils near Bytom, an area of Pb/ Zn mining and smelting in Upper Silesia, Poland, Applied
856 Geochemistry 1999; 14: 187-196.

857 US EPA. Standard operating procedure for GLNPO total alkalinity titration. . US EPA. Chicago 1992.

858 USGS. Lead-Rich Sediments, Coeur d'Alene River Valley, Idaho: Area, Volume, Tonnage and Lead
859 Content, 2001.

860 vanLoon GW, Duffy SJ. Environmental Chemistry. Oxford, UK: Oxford University Press, 2011.

861 Walling DE, Owens PN, Carter J, Leeks GJL, Lewis S, Meharg AA, et al. Storage of sediment-
862 associated nutrients and contaminants in river channel and floodplain systems. Appl. Geochem. 2003;
863 18: 195-220.

864 Wang L, Yu R, Hu G, Tu X. Speciation and assessment of heavy metals in surface sediments of
865 JinJiang River Tidal Reach, Southeast of China. Environ. Monit. Assess. 2010; 165: 491-499.

866 Wijayawardena MAA, Megharaj M, Naidu R. Bioaccumulation and toxicity of lead, influenced by
867 edaphic factors: using earthworms to study the effect of Pb on ecological health. J. Soils Sediments
868 2017; 17: 1064-1072.

869 Wilson B, Pyatt FB. Heavy metal dispersion, persistance, and bioccumulation around an ancient
870 copper mine situated in Anglesey, UK. Ecotoxicology and environmental safety 2007; 66: 224-231.

871 Wragg J, Palumbo-Roe B. Contaminant mobility as a result of sediment inundation: Literature review
872 and laboratory scale pilot study on mining contaminated sediments. British Geological Survey Open
873 Report, 2011, pp. 101.

874 Younger PL. Coalfield Abandonment: Geochemical processes and hydrochemical products. In:
875 Nicholson K, editor. Energy and the Environment: Geochemistry of fossil, nuclear and renewable
876 resources MacGregor Science, 1998, pp. 1-29.

877 Zakir HM, Shikazono N. Environmental Mobility and Geochemical Partitioning of Fe, Mn, Co, Ni, and
878 Mo in sediments of an Urban River. J. Environ. Chem. Ecotoxicol. 2011; 3: 116-126.

879 Zadnik T. Monitoring of lead in topsoil, forage, blood, liver and kidneys in cows in a lead polluted area
880 in Slovenia (1975-2002) and a case of lead poisoning (1993). International Journal of Chemical
881 Engineering 2010; 2010: 1-6.

882 Zhang X, Yang L, Li Y, Li H, Wang W, Ye B. Impacts of lead/zinc mining and smelting on the
883 environment and human health in China. Environ Monit Assess 2012; 184: 2261-2273.